Laminar Dispersion in Capillaries: Part IV. The Slug Stimulus

WILLIAM N. GILL and V. ANANTHAKRISHNAN

Clarkson College of Technology, Potsdam, New York

An exact analytical theory of the local behavior of finite slugs which are dispersed in three-dimensional velocity fields is developed. It is shown that the dispersion coefficient enters the problem as an eigenvalue. For the important special case of fully developed straight pipe flow, considered first by Taylor and later generalized by Aris, the dispersion coefficient can be found very easily by the present method, which also provides the basis for studying a large class of more complicated problems.

A detailed numerical analysis is carried out to determine the limits of applicability of the analytical theory. Fortunately, it is found that dispersion of slug stimuli in fully developed laminar tube flow is described by Equation (15) when τ exceeds certain minimum values which depend only weakly on Peclet number and are independent of slug length in the region considered here. Since peak mean concentrations are predicted accurately by Equation (19) for $X > 0.1$, this is a convenient quantity to use to determine dispersion coefficients experimentally.

On comparing the numerical and analytical results for local point concentrations, good agreement is found, provided the average concentration is predicted accurately by Equation (15). This is significant because it implies that a broad class of difficult transient heat and mass transfer problems, with aperiodic inlet disturbances, can be solved by using superposition in conjunction with the present approach.

Stimulus-response techniques for determining the flow characteristics of process vessels have been discussed extensively in recent years and a good summary of much of the work done in this field has been given recently by Levenspiel and Bischoff (9). One of the most common types of stimuli employed is the pulse or Dirac delta function which is an idealization that is useful in mathematical analysis but cannot actually be realized physically. In real systems, one must employ slugs of finite lengths and because of limitations inherent in measuring trace amounts accurately, one must often use slugs of substantial length. Thus it seems desirable to develop a rigorous theory which describes the local behavior of dispersing slugs, to compare the results obtained with other theoretical results in the literature, and to determine the limitations of the theory by testing it against both numerical and experimental data.

Taylor (*14*) was the first to present a mathematical analysis of the transient convective diffusion equation to describe dispersion in flow systems. Aris (*2*), Carrier (*5*), and Philip (*11*) generalized Taylor's work to include the effects of axial molecular diffusion and periodic inlet conditions, respectively. Bailey and Gogarty (3) and Ananthakrishnan, Gill, and Barduhn (*1, 8*) have presented detailed finite-difference solutions and the former also reported experimental data. Evans and Kenney (*6*) have reported experimental data which confirm the theory very well for very large values of dimensionless time τ. Gill (*7*) very recently has developed a local theory of Taylor diffusion in fully developed laminar tube flow with aperiodic conditions at the inlet of the tube.

The purposes of our work in this article are:

1. To develop an analytical theory which describes the local aspects of the transient dispersion of slugs in three-dimensional velocity fields wherein the velocity components are functions of r and ϕ. Also, it is shown that expressions for the dispersion coefficient now available in the literature for the special case of fully developed flow wherein $v = w = 0$ can be obtained easily by the present approach.
2. To integrate numerically the transient convective diffusion equation for a wide range of Peclet numbers and slug lengths to establish the general characteristics of dispersing slugs and to establish limits for the applicability of the analytical theory.
3. To examine existing experimental data carefully in terms of the detailed numerical results. Thus, where possible, parameter values used in the numerical calculations were chosen to correspond closely with those employed in experimental studies.

ANALYSIS

The present analysis of aperiodic systems will extend previous work (*7*) on step change inlet conditions to include finite slug inputs. Also it will be shown that the method of solution applies to systems with finite radial and angular velocity components which should be of practical interest since it is clear that transverse convection can alter the magnitude of longitudinal dispersion coefficients very markedly. For simplicity, we shall only consider cylindrical systems.

The convective diffusion equation written in cylindrical coordinates is

$$\frac{\partial C}{\partial t} + u(r,\phi)\frac{\partial C}{\partial x} + v(r,\phi)\frac{\partial C}{\partial r} + \frac{w(r,\phi)}{r}\frac{\partial C}{\partial \phi} = \frac{1}{r}\frac{\partial}{\partial r} r D_r(r,\phi)\frac{\partial C}{\partial r} + \frac{1}{r^2}\frac{\partial}{\partial \phi} D_\phi(r,\phi)\frac{\partial C}{\partial \phi} + \frac{\partial}{\partial x} D_x(r,\phi)\frac{\partial C}{\partial x} \quad (1)$$

and we have restricted attention to systems in which the components of the velocity vector are functions of r and ϕ, as are all the diffusion coefficients.

In dimensionless form Equation (1) is

$$\frac{\partial \theta}{\partial \tau} + u_1\frac{\partial \theta}{\partial X} + N_{Pe}\left[V_1\frac{\partial \theta}{\partial y} + \frac{w_1}{y}\frac{\partial \theta}{\partial \phi}\right] =$$

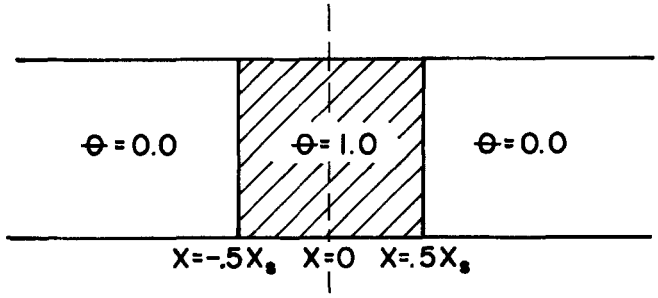

Fig. 1. Sketch of the capillary model with slug input.

$$\frac{1}{y}\frac{\partial}{\partial y}yD_1\frac{\partial\theta}{\partial y}+\frac{1}{y^2}\frac{\partial}{\partial\phi}D_2\frac{\partial\theta}{\partial\phi}+\frac{1}{N_{Pe}^2}\frac{\partial}{\partial X}D_3\frac{\partial\theta}{\partial X} \quad (2)$$

and the initial and boundary conditions are assumed to be

$$\begin{aligned}&\theta(0,X,y,\phi)=0, \quad X<-\tfrac{1}{2}X_s\\&\theta(0,X,y,\phi)=1, \quad -\tfrac{1}{2}X_s<X<\tfrac{1}{2}X_s\\&\theta(0,X,y,\phi)=0, \quad X>\tfrac{1}{2}X_s\\&\frac{\partial\theta}{\partial y}(\tau,X,1,\phi)=0\end{aligned} \quad (3)$$

and it is obvious that the dimensionless slug length X_s is a parameter of the problem.

The solution of Equation (2) is now formulated as a series expansion in $(\partial^k\theta_m/\partial X_1{}^k)$ where X_1 is the axial distance measured from a coordinate system which moves with the mean speed of flow U_m and is given by

$$X_1=X-\tau/2 \quad (4)$$

Then Equation (2) becomes

$$\frac{\partial\theta}{\partial\tau}+(u_1-\tfrac{1}{2})\frac{\partial\theta}{\partial X_1}+N_{Pe}\left[V_1\frac{\partial\theta}{\partial y}+\frac{w_1}{y}\frac{\partial\theta}{\partial\phi}\right]=\frac{1}{y}\frac{\partial}{\partial y}yD_1\frac{\partial\theta}{\partial y}+\frac{1}{y^2}\frac{\partial}{\partial\phi}D_2\frac{\partial\theta}{\partial\phi}+\frac{1}{N_{Pe}^2}\frac{\partial}{\partial X_1}D_3\frac{\partial\theta}{\partial X_1} \quad (5)$$

Now let

$$\theta=\theta_m+\sum_{k=1}^{\infty}f_k(\tau,y,\phi)\frac{\partial^k\theta_m}{\partial X_1{}^k} \quad (6)$$

where

$$\theta_m=\frac{1}{\pi}\int_o^{2\pi}\int_o^1 y\,\theta\,dy\,d\phi \quad (7)$$

If Equation (6) is substituted into Equation (5), the result is

$$\frac{\partial\theta_m}{\partial\tau}+(u_1-\tfrac{1}{2})\frac{\partial\theta_m}{\partial X_1}-\frac{D_3}{N_{Pe}^2}\frac{\partial^2\theta_m}{\partial X_1{}^2}+\sum_{k=1}^{\infty}\left\{\left[\frac{\partial f_k}{\partial\tau}+N_{Pe}\left(V_1\frac{\partial f_k}{\partial y}+\frac{w_1}{y}\frac{\partial f_k}{\partial\phi}\right)-\frac{1}{y}\frac{\partial}{\partial y}yD_1\frac{\partial f_k}{\partial y}-\frac{1}{y^2}\frac{\partial}{\partial\phi}D_2\frac{\partial f_k}{\partial\phi}\right]\frac{\partial^k\theta_m}{\partial X_1{}^k}+(u_1-\tfrac{1}{2})f_k\frac{\partial^{k+1}\theta_m}{\partial X_1{}^{k+1}}-\frac{D_3}{N_{Pe}^2}f_k\frac{\partial^{k+2}\theta_m}{\partial X_1{}^{k+2}}+f_k\frac{\partial^{k+1}\theta_m}{\partial\tau\partial X_1{}^k}\right\}=0 \quad (8)$$

If the process of distributing θ_m is assumed to be diffusive in nature, then one can write

$$\frac{\partial\theta_m}{\partial\tau}=K\frac{\partial^2\theta_m}{\partial X_1{}^2} \quad (9)$$

which requires that

$$\frac{\partial^{k+1}\theta_m}{\partial\tau\partial X_1{}^k}=K\frac{\partial^{k+2}\theta_m}{\partial X_1{}^{k+2}} \quad (10)$$

Equations (9) and (10) can be substituted into (8) and one gets

$$\left[\frac{\partial f_1}{\partial\tau}+N_{Pe}\left(V_1\frac{\partial f_1}{\partial y}+\frac{w_1}{y}\frac{\partial f_1}{\partial\phi}\right)+(u_1-\tfrac{1}{2})-\frac{1}{y}\frac{\partial}{\partial y}yD_1\frac{\partial f_1}{\partial y}-\frac{1}{y^2}\frac{\partial}{\partial\phi}D_2\frac{\partial f_1}{\partial\phi}\right]\frac{\partial\theta_m}{\partial X_1}+\left[\frac{\partial f_2}{\partial\tau}+N_{Pe}\left(V_1\frac{\partial f_2}{\partial y}+\frac{w_1}{y}\frac{\partial f_2}{\partial\phi}\right)+(u_1-\tfrac{1}{2})f_1+\left(K-\frac{D_3}{N_{Pe}^2}\right)-\frac{1}{y}\frac{\partial}{\partial y}yD_1\frac{\partial f_2}{\partial y}-\frac{1}{y^2}\frac{\partial}{\partial\phi}D_2\frac{\partial f_2}{\partial\phi}\right]\frac{\partial^2\theta_m}{\partial X_1{}^2}+\sum_{k=1}^{\infty}\left[\frac{\partial f_{k+2}}{\partial\tau}+N_{Pe}\left(V_1\frac{\partial f_{k+2}}{\partial y}+\frac{w_1}{y}\frac{\partial f_{k+2}}{\partial\phi}\right)+(u_1-\tfrac{1}{2})f_{k+1}+\left(K-\frac{D_3}{N_{Pe}^2}\right)f_k-\frac{1}{y}\frac{\partial}{\partial y}yD_1\frac{\partial f_{k+2}}{\partial y}-\frac{1}{y^2}\frac{\partial}{\partial\phi}D_2\frac{\partial f_{k+2}}{\partial\phi}\right]\frac{\partial^{k+2}\theta_m}{\partial X_1{}^{k+2}}=0 \quad (11)$$

If Equation (11) is satisfied by equating the coefficients of $(\partial^k\theta_m/\partial X_1{}^k)$ to zero, then the following system of equations is generated

$$\frac{\partial f_1}{\partial\tau}+N_{Pe}\left(V_1\frac{\partial f_1}{\partial y}+\frac{w_1}{y}\frac{\partial f_1}{\partial\phi}\right)+(u_1-\tfrac{1}{2})=\frac{1}{y}\frac{\partial}{\partial y}yD_1\frac{\partial f_1}{\partial y}+\frac{1}{y^2}\frac{\partial}{\partial\phi}D_2\frac{\partial f_1}{\partial\phi} \quad (12a)$$

$$\frac{\partial f_2}{\partial\tau}+N_{Pe}\left(V_1\frac{\partial f_2}{\partial y}+\frac{w_1}{y}\frac{\partial f_2}{\partial\phi}\right)+(u_1-\tfrac{1}{2})f_1+\left(K-\frac{D_3}{N_{Pe}^2}\right)=\frac{1}{y}\frac{\partial}{\partial y}yD_1\frac{\partial f_2}{\partial y}+\frac{1}{y^2}\frac{\partial}{\partial\phi}D_2\frac{\partial f_2}{\partial\phi} \quad (12b)$$

$$\frac{\partial f_{k+2}}{\partial\tau}+N_{Pe}\left(V_1\frac{\partial f_{k+2}}{\partial y}+\frac{w_1}{y}\frac{\partial f_{k+2}}{\partial\phi}\right)+(u_1-\tfrac{1}{2})f_{k+1}+\left(K-\frac{D_3}{N_{Pe}^2}\right)f_k=\frac{1}{y}\frac{\partial}{\partial y}yD_1\frac{\partial f_{k+2}}{\partial y}+\frac{1}{y^2}\frac{\partial}{\partial\phi}D_2\frac{\partial f_{k+2}}{\partial\phi},\quad k=1,2\ldots,\infty \quad (12c)$$

Equations (12a), (12b), and (12c) together with the boundary conditions

$$f_k(0,y,\phi)=0 \quad (13a)$$

$$\frac{\partial f_k}{\partial y}(\tau,1,\phi)=0 \quad (13b)$$

and the condition

$$\int_o^1 yf_k\,dy=0$$

which follows from Equations (6) and (7), form the basis for studying a variety of dispersion problems. Some of the most important of these dispersion problems are related to fully developed flow in a straight tube; fully developed flow in a curved tube; and fully developed flow between rotating concentric cylinders.

In the present paper we shall examine in detail only the dispersion of slugs in straight tubes. Steady state heat transfer in curved pipes has recently been studied by Mori and Nakayama (*10*) and the transient mass dispersion analog of this problem is being studied currently at Clarkson.

In the special case of fully developed flow in a straight pipe, then $v = w = 0$, and if the fluid is initially distributed uniformly over a cross section, as was assumed in writing Equations (3), then derivatives with respect to ϕ are zero and we get as a final system of equations

$$\frac{\partial f_1}{\partial \tau} + (u_1 - \tfrac{1}{2}) - \frac{1}{y}\frac{\partial}{\partial y} y D_1 \frac{\partial f_1}{\partial y} = 0 \qquad (14a)$$

$$\frac{\partial f_2}{\partial \tau} + (u_1 - \tfrac{1}{2}) f_1 + \left(K - \frac{D_3}{N_{Pe}^2}\right) - \frac{1}{y}\frac{\partial}{\partial y} y D_1 \frac{\partial f_2}{\partial y} = 0 \qquad (14b)$$

$$\frac{\partial f_{k+2}}{\partial \tau} + (u_1 - \tfrac{1}{2}) f_{k+1} + \left(K - \frac{D_3}{N_{Pe}^2}\right) f_k - \frac{1}{y}\frac{\partial}{\partial y} y D_1 \frac{\partial f_{k+2}}{\partial y} = 0 \qquad (14c)$$

and because of symmetry

$$\frac{\partial f_k}{\partial y}(\tau, 0, \phi) = 0$$

The solution of Equations (14) together with Equation (15)

$$\theta_m = \tfrac{1}{2}\,\mathrm{erf}\left[\frac{\tfrac{1}{2}X_s - (X - \tfrac{1}{2}\tau)}{\sqrt{4K\tau}}\right] + \tfrac{1}{2}\,\mathrm{erf}\left[\frac{\tfrac{1}{2}X_s + (X - \tfrac{1}{2}\tau)}{\sqrt{4K\tau}}\right] \qquad (15)$$

which is the solution of Equation (9) and satisfies the conditions at $\tau = 0$ in Equations (3), constitutes the analytical solution of the dispersion problem with a slug stimulus. The solution applies for large values of τ and is exact in the limit $\tau \to \infty$. However, it will be shown that for practical purposes the solution is useful for fairly small values of τ and the magnitudes of the minimum values of τ above which the solution is valid will be given in this paper.

If the flow is laminar, D_1 and D_3 are unity and it is easily shown that the parts of f_1 and f_2 which depend on y only are given by

$$f_{1s} = \frac{1}{8}\left[-\frac{1}{3} + y^2 - \frac{y^4}{2}\right] \qquad (16a)$$

$$f_{2s} = \frac{1}{128}\left[\frac{1}{8}y^8 - \frac{5}{9}y^6 + \frac{5}{6}y^4 - \frac{1}{2}y^2 + \frac{31}{360}\right] \qquad (16b)$$

In solving for f_2 one finds that $(\partial f_2/\partial y)(\tau, 1) = 0$ if, and only if

$$K = \frac{1}{N_{Pe}^2} - 2\int_0^1 y(\tfrac{1}{2} - y^2) f_{1s}\, dy = \frac{D}{a^2 u_o^2}\left[D + \frac{a^2 u_o^2}{192\, D}\right] \qquad (17)$$

Thus K plays the role of an eigenvalue in this solution. Equations (16) and (17) are the same results as Taylor (*14*) and Aris (*2*) found by entirely different approaches than the one used in the present study. The nature of the solutions to Equations (14) is discussed in more detail in reference 7.

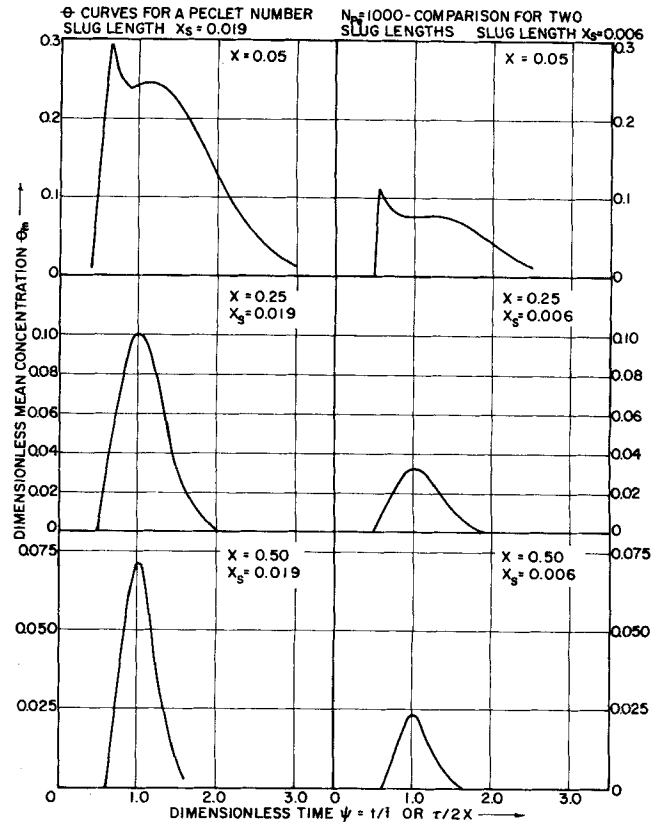

Fig. 2. Comparison of C curve for different slug lengths at N_{Pe} = 1,000.

If the flow is not laminar and D_1 and D_3 are functions of y, then by integrating Equation (14*b*) it is easy to show that $(\partial f_2/\partial y)(\tau, 1) = 0$, if and only if, the dispersion coefficient is

$$K = 2\left[\int_0^1 (D_3/N_{Pe}^2)\, dy - \int_0^1 (u_1 - \tfrac{1}{2}) y f_{1s} dy\right] \qquad (18)$$

and the local concentration profiles can be obtained by integrating Equations (14). Of course the special case described by Equation (18) is the same as the results one would get by using the method of moments as Aris did.

NUMERICAL ANALYSIS

For the case of laminar fully developed flow, Equation (1), with the auxiliary conditions given in Equations (3) and illustrated in Figure 1, was integrated by the implicit finite-difference scheme discussed in Parts I and II of this series. This was done to obtain detailed information on the behavior of slugs in a prescribed velocity field and perhaps, more importantly, to determine the limits on τ within which the analytical theory is valid.

Numerical solutions have been obtained for:

1. Peclet numbers of 1,000 and 325 with a slug length of 20.4 cm., which corresponds to Bournia's (*4*) experimental condition. The tube radius in his case was a = 1.085 cm. and for the N_{Pe} studied, X_s = 0.019 and 0.058 respectively.

2. Peclet numbers of 192, 24, and 10 with a slug length of 0.24a, where a is the radius of the tube so that X_s equals 0.00125, 0.01, and 0.024. This shorter slug length was used because low Peclet number results are very inconvenient to obtain for Bournia's experimental system since the corresponding dimensionless slug length is too

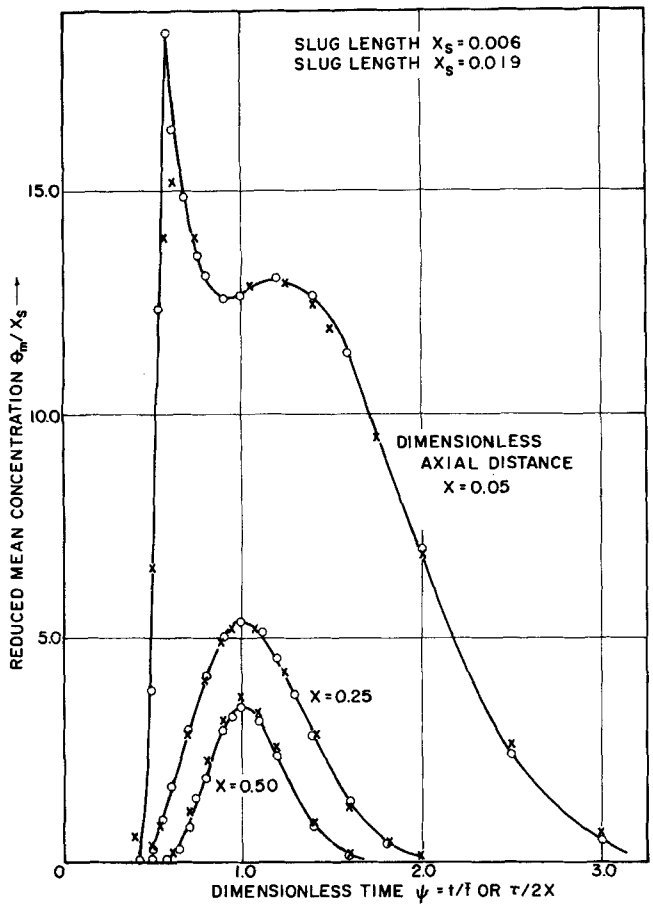

Fig. 3. Comparison of $\theta m/X_S$ vs. ψ plot (reduced C curve) for two different slug lengths for N_{Pe} = 1,000. Note that curves are essentially independent of slug length.

large for the available computer memory locations, even in a large digital computer, and the computations would be inordinately difficult to perform.

3. Peclet number of 1,000 for X_s equal 0.019 and 0.006 to establish, with other parameters fixed, the effect of slug length on the range of applicability of the dispersion model. In these cases, solutions have been obtained up to τ values of 1.60 and 5.00, which are high enough so that the dispersion model is valid.

Bournia et al. have presented the bulk of their results in terms of peak mean concentration θ_{pm}, which is the maximum concentration of tracer material that passes a specified observation point. In other words, it is the peak concentration of the C curve. The advantage of using this quantity is that the dispersion coefficient can be evaluated in a very simple manner when Equation (15) is valid. In this case the peak mean concentration will pass the analysis point at the mean residence time $\bar{t} = x/U_m$, and hence

$$\theta_{pm} = \text{erf}\left[\frac{X_s}{4}\,\frac{1}{\sqrt{2KX}}\right] \qquad (19)$$

With the exception of K, all the quantities in Equation (19) are known and thus K can be calculated very easily.

DISCUSSION OF RESULTS

It was found that the system behavior is essentially independent of the slug length for the range considered here. This is clearly seen in Figure 2 where the C curves are plotted for two different slug lengths of $19a$ and $6a$ (where a is the radius of the tube), for a Peclet number N_{Pe} of 1,000 and different observation points, X = 0.05, 0.25, and 0.50. In the plots of C curves, ψ is the reduced time $t/\bar{t}$ and in the dimensionless variables used in this study ψ is $\tau/2X$. At a Peclet number of 1,000, the observation point in Bournia's experiments was X = 0.23.

It is seen in Figure 2 that the C curves for the two slug lengths behave in a very similar fashion at each of the different values of X. If the argument is small enough, the first term of the series expansion of the error function will dominate and then Equation (19) suggests that the peak mean concentration scaled by X_s, θ_{pm}/X_s, is independent of slug length. From the numerical results it is found that the ratio of the peak mean concentration θ_{pm} is equal to the ratio of the slug lengths. For example, for the case of X = 0.25, θ_{pm}, for the slug length $X_s = 19a$ is 0.101 and for $X_s = 6a$, θ_{pm} = 0.032, so that the ratios of slug lengths and peak mean concentrations are both equal to 3.16. This can easily be verified for all the three cases illustrated.

Furthermore, it was found that not only the peak mean concentration, but also the entire concentration distribution given by the C curves, is directly proportional to the slug length. This is shown in Figure 3, which is a plot of θ_m/X_s vs. dimensionless time ψ. It can be seen from the figure that for each of the dimensionless lengths plotted, the concentration distributions are essentially identical for the two slug lengths X_s = 0.006 and 0.019. This shows to a good approximation that, essentially independent of the slug length, for the same Peclet number and observation point X, the properly scaled residence time distributions are almost the same.

Figure 4 shows C curves plotted for the same slug length of $0.24a$ but for two different N_{Pe} of 192 and 10. It can be seen that the variance, or spread, of the residence time distributions increases with a decrease in Peclet number. This occurs because axial molecular diffusion becomes more significant at lower N_{Pe} and this in-

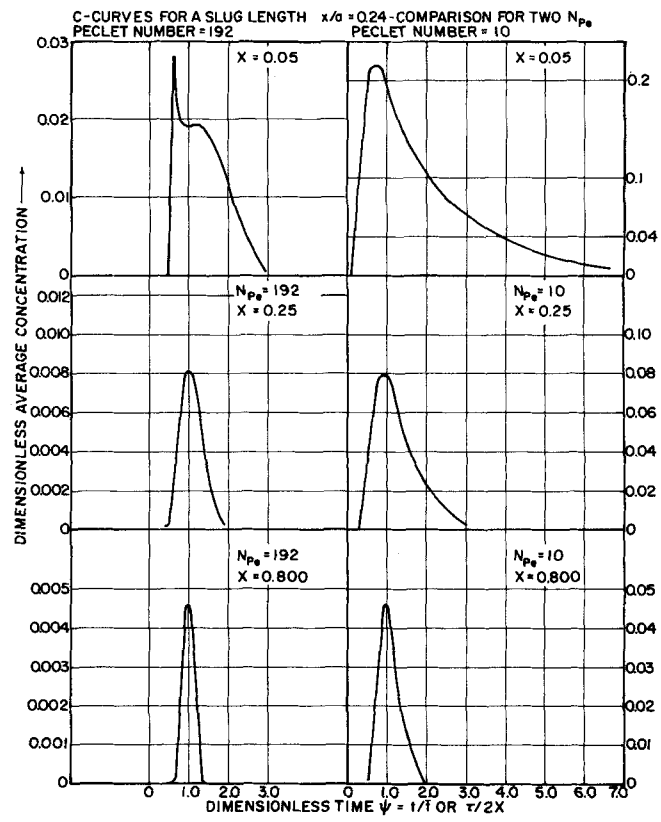

Fig. 4. Comparison of C curves for high and low N_{Pe} for slug length x_s/a = 0.24.

TABLE 1. MINIMUM VALUES OF τ FOR THREE SYSTEMS

Peclet No.	Slug	τ_{min} above which Equation (15) is valid: Step change	Case B, Part II
>100	0.600	0.8	0.8
25	0.500	1.25	1.25
10	0.300	1.75	0.50

creases the dispersion or the spread. As in the case of a step change, it was verified that axial molecular diffusion is negligible for $N_{Pe} > 100$ and in the range $100 < N_{Pe} < \infty$, the concentration distributions are identical for all practical purposes.

Another point that can be observed from Figures 2, 3, and 4 is that at very short distances and high Peclet numbers, the C curve has two peaks. Similar behavior is also seen in the θ_m vs. X/τ plot for small values of time τ and high N_{Pe}, as shown in Figure 5. It was found that for all the high Peclet numbers investigated, at very small times the solutions agree with the pure convection solution given by Taylor. As the value of τ increases, and dispersion no longer takes place only by pure convection, the concentration distributions evidence two peaks as in Figure 5 and this behavior continues up to a τ value of about 0.25.

As τ increases further, the θ_m distribution eventually becomes symmetrical according to Equation (15) and is due to the combined mechanisms of axial convection and radial and axial molecular diffusion. The concentration distribution tends to a Gaussian error function and Figures 2 and 4 depict this phenomenon. It is seen that as X increases, the C curves tend to become symmetrical for both high and low Peclet numbers. At a dimensionless distance $X = 0.800$, the distributions have become error function curves, which, to a good approximation, correspond to the solution given by Equation (15).

Table 1 shows for different Peclet numbers the approximate values of τ above which the numerical solution follows Equation (15). These data are valid for all the slug lengths studied here.

A significant result that can be seen from Table 1 is that the τ_{min} required for the dispersion model to be valid are far lower than those required in case of a step change input. The slug input resembles the case B inlet condition discussed in Part II, in which case a similar trend was observed. In fact, the case B inlet condition can be viewed as representing an indefinitely long slug. Since the τ_{min} requirements in the cases considered in the present study are even less than those required for the case B inlet condition, it is clear that slug length should be taken into consideration as X_s gets large. This behavior is significant since the use of relatively short slugs can extend the range of applicability of the dispersion model, particularly in the low Peclet number region.

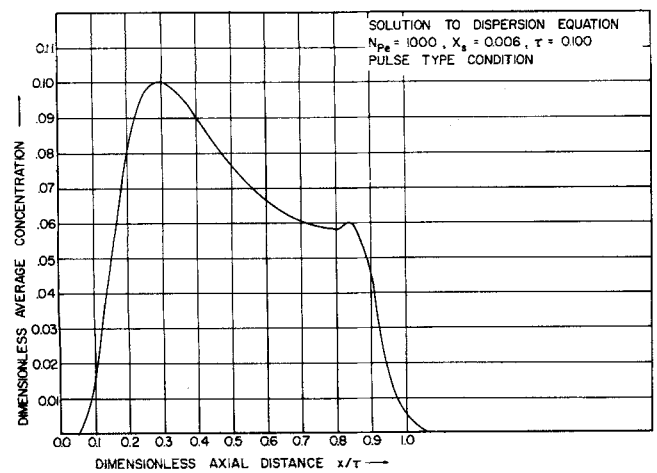

Fig. 5. Solution to laminar dispersion equation with a slug input for a capillary model, N_{Pe} = 1,000, dimensionless slug length X_s = 0.006, dimensionless time τ = 0.100. The broken line represents the pure convection solution.

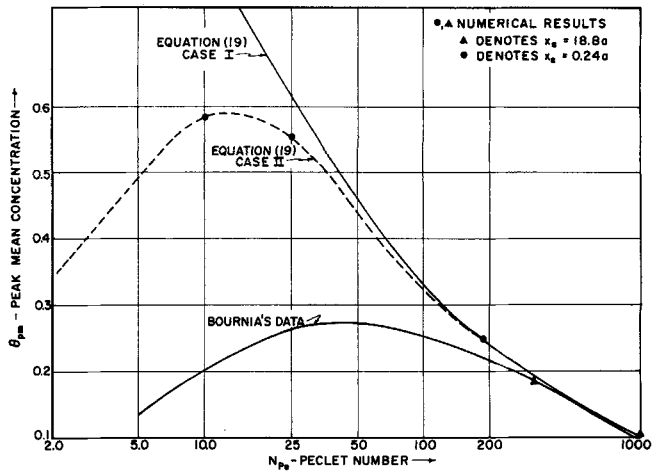

Fig. 6. Comparison of numerical peak mean concentration results with the results of Bournia et al with Equation (19). Case I denotes no axial diffusion; Case II denotes axial diffusion included.

Figure 6 represents a plot of peak mean concentration θ_{pm} vs. Peclet number at x = 250 cm. and x_s = 20.4 cm. which corresponds to the experiments of Bournia et al. as plotted in their Figure 3. It is seen that the numerical results at N_{Pe} = 1,000 and 325 agree extremely well with the analytical solution, and as N_{Pe} gets smaller Bournia's results deviate significantly from the solution given in Equation (19). In contrast, the comprehensive data of Evans and Kenney (*6*) for gases, taken at x = 1729 cm. and x_s = 0.683 cm., agree with Equation (15), and therefore Equation (19), as precisely as one can read their Figure 2, over the entire range of N_{Pe} that they studied and this included N_{Pe} less than 5. The experiments of Reejhsinghani et al. (*12, 13*), which correspond to indefinitely long slugs of liquid, are also in excellent agreement with the analytical theory as long as natural convection was negligible and this included runs at N_{Pe} = 45.

Bournia's data are shown in Figure 6 primarily to illustrate the possible effect of natural convection on the dispersion of slugs in gas phase systems.

As suggested in Part I and discussed in more detail in

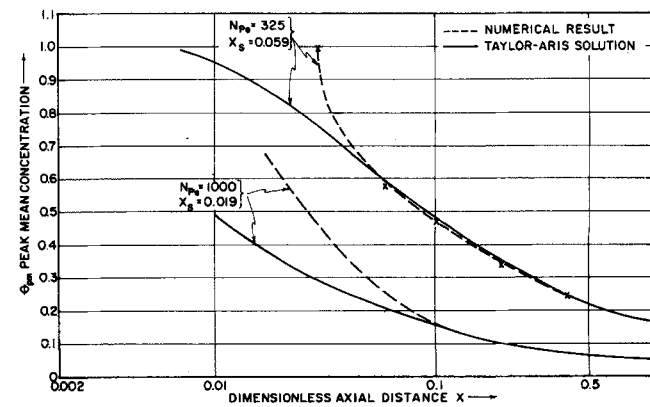

Fig. 7. Comparison of numerical peak mean concentration results with Equation (19).

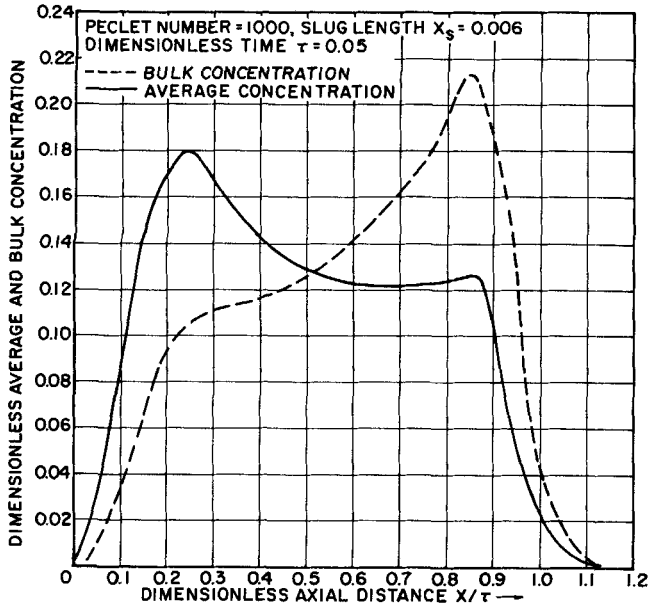

Fig. 8a. Comparison of average and bulk concentration distributions for N_{Pe} = 1,000, slug length X_s = 0.006, and dimensionless time τ = 0.05.

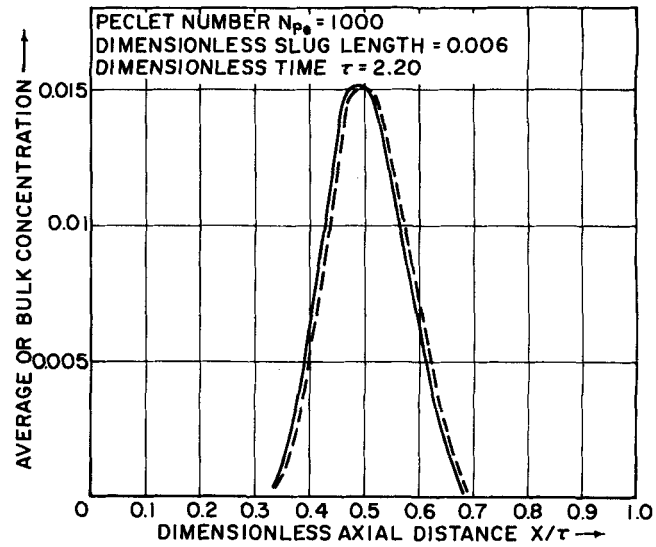

Fig. 8b. Comparison of average and bulk concentrations for N_{Pe} = 1,000, X_s = 0.006, and τ = 2.20.

Part III, the markedly greater dispersion in Bournia's experiments over that predicted by Equation (17) is caused by the effect of natural convection. This is clear when one notes that the Grashoff number is estimated to be on the order of 14,000 in their run at N_{Pe} = 12.5 wherein the dispersion coefficient was observed to be 8.5 times that predicted by Equation (17). The experiments in Part V of this series are aimed at determining the effects of natural convection in vertical tubes and they show clearly, by varying the Grashoff number systematically, that under such conditions natural convection may have very large effects on dispersion even with small differences in density.

Qualitatively one can visualize the effect of natural convection on a slug which is lighter than the carrier fluid as follows: At the start of the dispersion process, when τ is small, pure convection predominates and the slug and carrier fluids are distributed primarily by the parabolic velocity field. That is, for short times before molecular diffusion is significant, the slug behaves essentially as a rigid body paraboloid finger which grows and displaces the carrier fluid in front of it. Similarly the carrier fluid behind the slug displaces it in the same fashion. Consequently the faster moving part of the forward portion of the slug enriches the center of the tube with light fluid. This fluid is accelerated by buoyancy forces which thereby elongate the velocity profile in the front portion of the slug. Conversely, in the trailing portion of the slug the center of the tube is richer in heavier carrier fluid which is displacing the slug. Thus the action of gravity in this region tends to retard the center and accelerate the region near the wall which flattens the velocity profile. The net result is that the band occupied by the lighter slug spreads out more rapidly because of the action of buoyancy forces. This is discussed in detail in Part V.

Numerical solutions could not be computed conveniently for low N_{Pe} for slug lengths of x_s = 20.4 cm. because the corresponding dimensionless slug length is too large and the calculation is impractical. But since it was found that the dispersion behavior is essentially independent of slug length as shown in Figure 3, low Peclet number results were obtained for smaller slug lengths to determine their agreement with Equation (19). It is seen that the numerical results are in excellent agreement with Equation (19) and both agree with Evans and Kenney's experiments over the entire range of N_{Pe} from 10 to 1,000. To illustrate the importance of axial molecular diffusion, the result which neglects this effect is also included in Figure 6. As one would expect, the effect of axial molecular diffusion becomes important for $N_{Pe} < 100$.

Figure 7 shows typical results of θ_{pm} vs. X, and in both of these cases it can be seen that the dispersion model predicts the correct θ_{pm} for all X greater than about 0.1. A similar plot for N_{Pe} = 10 indicates much the same behavior with the dispersion model yielding accurate results for $X > 0.1$.

Along with average concentrations, values of bulk concentrations θ_b are of interest and a comparison of the two is given in Figures 8a and 8b for N_{Pe} = 1,000, X_s = 0.006, and for values of τ equal 0.05 and 0.5. It is seen that for short times, the bulk concentration distribution also shows two peaks but the higher peak occurs at significantly different values of X for the two cases. As time increases, both the average and the bulk concentration distributions approach each other more closely as seen in Figure 8b. Obviously, it makes little difference whether one is discussing average or bulk mean concentration distributions in cases corresponding to Figure 8b, whereas the distributions are fundamentally different at small values of time.

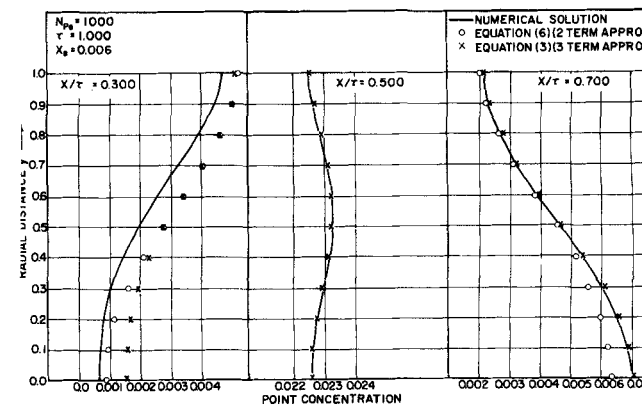

Fig. 9. Comparison of local point concentration distributions predicted by two and three terms of Equation (6) with exact numerical solution.

In Figure 9 a comparison is made between local concentration distributions determined numerically and those obtained from Equation (6) by using two and three terms of the series. At $X/\tau = 0.5$ and 0.700 the analytical and numerical results agree extremely well. Also, at $X/\tau = 0.7$ it can be seen that the third term adds a correction which improves the analytical solution significantly. The reason for the discrepancies at $X/\tau = 0.3$ is that θ_m, which is the first term of Equation (6), is predicted by the numerical solution and by Equation (15) to be 3.0×10^{-3} and 3.8×10^{-3}, respectively. The shapes of the three-term approximation and the numerical solution are very similar. They differ by an almost constant amount equal to 0.8×10^{-3} and therefore would agree well if the value 3×10^{-3} is used for θ_m. It is found in general that the differences between Equation (15) and the numerical solution are a maximum at the rear end of the slug and for the slug depicted in Figure 9 the point $X/\tau = 0.3$ is close to the tail.

CONCLUSIONS

1. The analytical theory provides a basis for studying dispersion in some three-dimensional flows. It is a significant simplification to reduce the three-dimensional transient problem to that of finding the two-dimensional f_k functions. In any event, the crucial calculation is the determination of the dispersion coefficient K, and this requires one to solve only the two-dimensional steady state problem for f_{2s}. The nature of the specific problem to be solved will determine if additional simplifying assumptions, such as boundary-layer approximations, can be made.

2. Equation (15) predicts the average concentration distribution of dispersing slugs quite well when values of τ exceed those in Table 1. The maximum differences between the analytical and numerical results invariably occur near the tail of the slug. In this region Equation (15) predicts values which are conservative since they are slightly higher than the numerical results. Values of the peak mean concentrations determined numerically and from Equation (15) are in excellent agreement over the entire range of parameters studied provided $X > 0.1$.

3. The local radial concentration distributions predicted by the analytical theory are accurate whenever the average concentration at the corresponding cross section is predicted accurately by Equation (15).

4. For the slug lengths considered here, which correspond to the range normally encountered in experiments, the properly scaled concentration distribution of the dispersing slug is essentially independent of slug length. This is true even for small values of dimensionless time, before Equation (15) applies, and in this region the C curves exhibit twin peaks if the Peclet number is large so that axial molecular diffusion is negligible. However, as X_s gets very large the slug stimulus approaches the case B condition studied in Part II and there is, no doubt, a critical value of X_s above which the function θ_m/X_s is no longer independent of X_s.

ACKNOWLEDGMENT

This work was sponsored in part by the Office of Saline Water, U.S. Department of Interior. The numerical calculations were done at the Computing Center of The State University of New York at Buffalo.

NOTATION

a = tube radius
C = concentration
C_o = initial concentration in slug
D = molecular diffusion coefficient
D_1 = dimensionless diffusion coefficient D_r/D
D_2 = dimensionless diffusion coefficient D_ϕ/D
D_3 = dimensionless diffusion coefficient D_x/D
D_ϕ = total diffusion coefficient in ϕ direction
D_r = total diffusion coefficient in r direction
D_x = total diffusion coefficient in x direction
f_k = functions defined by Equations (6), (12), and (13)
f_{ks} = asymptotic form of f_k for $\tau \to \infty$
K = dispersion coefficient
N_{Pe} = Peclet number, $u_o a/D$
r = radial coordinate measured from center of tube
t = time
$\bar{t}$ = mean residence time
u = axial velocity component, x direction
u_1 = dimensionless axial velocity
u_o = reference velocity. Centerline velocity for case of Poiseuille flow; $u_o = 2U_m$
U_m = mean speed of flow in axial direction
v = radial velocity component
V_1 = dimensionless radial velocity, V/u_o
w = angular velocity component
w_1 = dimensionless angular velocity component, w/u_o
X = x/aN_{Pe}
X_1 = $(X - \tau/2)$
X_s = dimensionless slug length x_s/aN_{Pe}
x = axial coordinate
x_s = slug length
y = dimensionless radial coordinate, r/a

Greek Letters

τ = dimensionless time tD/a^2
ϕ = angular coordinate
θ = dimensionless concentration C/C_o
θ_b = dimensionless bulk mean concentration, $\theta_b = 4\int_0^1 y\, u_1\, \theta\, dy$
θ_{pm} = dimensionless peak mean concentration
θ_m = dimensionless mean concentration defined by Equation (7)
ψ = reduced time, $\psi = t/\bar{t} = \tau/2X$
Σ = summation sign

LITERATURE CITED

1. Ananthakrishnan, V., W. N. Gill, and A. J. Barduhn, *AIChE J.*, **11**, 1063 (1965).
2. Aris, Rutherford, *Proc. Roy. Soc. (London)*, **252A**, 538 (1959).
3. Bailey, H. R., and W. B. Gogarty, *ibid.*, **259A**, 352 (1962).
4. Bournia, A., J. Coull, and G. Houghton, *ibid.*, **261A**, 227 (1961).
5. Carrier, G. F., *Quart. Appl. Math.*, **14**, 108 (1956).
6. Evans, E. V., and C. N. Kenney, *Proc. Roy. Soc. (London)*, **284A**, 540 (1965).
7. Gill, W. N., *Proc. Roy. Soc. (London)*, **A298**, 335 (1967).
8. ———, and V. Ananthakrishnan, *AIChE J.*, **12**, 906 (1966).
9. Levenspiel, Otto, and K. B. Bischoff, "Advances in Chemical Engineering," Vol. 4, pp. 98-198, Academic Press, New York (1963).
10. Mori, Yasuo, and Wataru Nakayama, *Intern. J. Heat Mass Transfer*, **8**, 67 (1965).
11. Philip, J. R., *Australian J. Phys.*, **16**, 287 (1963).
12. Reejhsinghani, N. S., W. N. Gill, and A. J. Barduhn, *AIChE J.*, **12**, 916 (1966).
13. Reejhsinghani, N. S., A. J. Barduhn, and W. N. Gill, paper presented at AIChE Detroit meeting (1966).
14. Taylor, G. I., *Proc. Roy. Soc., (London)*, **219A**, 186 (1953).

Manuscript received August 25, 1966; revision received December 5, 1966; paper accepted December 12, 1966. Paper presented at AIChE Detroit meeting.